JOURNAL OF SPACECRAFT AND ROCKETS
Vol. 55, No. 5, September–October 2018

Engineering Notes

General Hinged Rigid-Body Dynamics Approximating First-Order Spacecraft Solar Panel Flexing

Cody Allard,* Hanspeter Schaub,† and Scott Piggott‡
University of Colorado, Boulder, Colorado 80309-0431

DOI: 10.2514/1.A34125

Nomenclature

B_c, S_i	=	rigid hub center of mass location and ith solar panel center of mass location, respectively
$\{\hat{\boldsymbol{b}}_1, \hat{\boldsymbol{b}}_2, \hat{\boldsymbol{b}}_3\}$	=	body frame basis vectors
$\boldsymbol{c}$	=	vector from point B to center of mass of the spacecraft C, m
c_i, θ_i	=	ith solar panel torsional damping, $(\mathrm{N}\cdot\mathrm{m}\cdot\mathrm{s})/\mathrm{rad}$; and deflection from equilibrium, deg, respectively
d_i, k_i	=	ith solar panel center of mass offset, m; and torsional spring constant, $(\mathrm{N}\cdot\mathrm{m})/\mathrm{rad}$, respectively
$\boldsymbol{F}_{\text{ext}}$	=	vector sum of external forces on spacecraft, N
$\boldsymbol{H}_{\text{sc},B}$	=	angular momentum vector of spacecraft about point B, $\mathrm{N}\cdot\mathrm{m}\cdot\mathrm{s}$
$\{\hat{\boldsymbol{h}}_{i,1}, \hat{\boldsymbol{h}}_{i,2}, \hat{\boldsymbol{h}}_{i,3}\}$	=	ith hinge frame basis vectors
$[I_{\text{sc},B}]$, $[I_{\text{sp}_i,S_i}]$	=	inertia tensor of spacecraft about point B and of solar panel about point S_i, $\mathrm{kg}\cdot\mathrm{m}^2$, respectively
$\boldsymbol{L}_B$	=	vector of sum of external torques of spacecraft about point B, $\mathrm{N}\cdot\mathrm{m}$
m_{sc}, m_{hub}, m_{sp_i}	=	mass of spacecraft, hub, and ith solar panel, respectively
N, B, H_i	=	inertial frame origin, body frame origin, and ith hinge frame origin, respectively
$\mathcal{N}$, $\mathcal{B}$, $\mathcal{H}_i$, $\mathcal{S}_i$	=	reference frame of inertial, body, ith hinge, and ith solar panel, respectively
$\boldsymbol{r}_{B/N}$	=	position vector of B with respect to N, m
$\{\hat{\boldsymbol{s}}_{i,1}, \hat{\boldsymbol{s}}_{i,2}, \hat{\boldsymbol{s}}_{i,3}\}$	=	ith solar panel frame basis vectors
$\boldsymbol{\omega}_{\mathcal{B}/\mathcal{N}}$	=	angular velocity vector of $\mathcal{B}$ frame with respect to $\mathcal{N}$ frame, deg/s

I. Introduction

SPACECRAFT designs include a range of shapes and sizes, as well as deployable structural components such as large solar panels or antennas. Typically, these components are connected to the spacecraft as cantilevered elements; therefore, they are susceptible to flexing behavior. In many situations, this behavior needs to be included in the dynamics. The spacecraft is typically assumed to be a rigid body in initial modeling, but this assumption degrades the fidelity of the simulation if there are components that flex. Flexible dynamics impacts both the translational and rotational motions (and associated stability margins) of the spacecraft, as well as sensor modeling such as accelerometers and rate gyroscopes. For simulation and analysis purposes, flexing is very important because it can impact the performance, requirements, and success of the mission.

There are many different ways to model flexible dynamics [1]. One method is to assume that the primary impact will be on the attitude dynamics of the spacecraft so that the translational motion coupling is ignored [2]. Also, in some scenarios, the effects of flexible behavior can be assumed to only impact one plane of motion [2–4]. These methods are helpful in the early stages of a mission, but they lack fidelity and are limited in application, in that they do not allow general three-dimensional closed-loop dynamics to be considered.

The field of multibody dynamics has received extensive research in modeling flexible dynamics, and the equations of motion presented are generalized for complex and diverse problems [1,5]. This results in rederivation of equations because of generality [6–12]. These methods are required for unique and complex systems because the equations of motion depend on how many joints are interconnected. For example, in robotic systems, the number of interconnected joints varies widely, and the equations of motion are specific to that system [13,14]. Because there are many spacecraft that have similar designs with appended rigid bodies, there is a need to develop equations of motion that can be readily applied to these spacecraft. However, as is illustrated in this Note, deriving complete equations of motion for a general spacecraft configuration is a challenging and time-consuming task.

Related to the work in this Note, multiple publications presented models of spacecraft dynamics with appended solar panels [15–17]. However, this previous research was mainly focused on the deployment of solar panels and how the deployment affected the dynamics of the spacecraft [15–17]. Also, the previous research on deployable solar panels was specific to solar panels that were composed of interconnected bodies. This Note considers systems in which the solar panels are single rigid bodies.

Additionally, there was extensive research on the attitude control of flexible spacecraft and spacecraft structures. This area of research used dynamics formulations for the flexing phenomenon; therefore, the literature introduced many different ways to model flexible dynamics. Sometimes, a new control algorithm, for proof of concept, will assume the primary impact of flexing is constrained to one body axis, which greatly simplifies the flexible dynamics formulation [4,18]. Another common strategy is to assume that the flexible dynamics can be added on as an external perturbation to the spacecraft with modal coordinate dynamics [19–21]. However, the dynamics formulations either make too many assumptions that limit the applicability of the solution, energy and momentum verification is not available, or the focus of the work is not on the dynamics and further work must be done to implement the solution in simulation software.

When developing equations of motion of multibody systems, an important consideration is determining what analytical method to use to arrive at the equations. Lagrangian mechanics [3,4,22–24], Newtonian and Eulerian mechanics [2,25], and Kane's method [26,27] are the three most common methods for spacecraft. Each have their advantages and disadvantages [22]; in some situations, a certain method can be more beneficial than the others. For example, the Lagrangian approach is a desirable method based on the simple form of the method; however, special identities and algebraic manipulation are required to convert from generalized coordinates and quasi velocities to the desired angular velocity vector form [23,24]. In this

Received 23 October 2017; revision received 25 April 2018; accepted for publication 7 May 2018; published online 13 August 2018.

*Graduate Research Assistant, Department of Aerospace Engineering Sciences, 431 UCB, Colorado Center for Astrodynamics Research. Student Member AIAA.

†Professor, Glenn L. Murphy Endowed Chair, Department of Aerospace Engineering Sciences, Laboratory for Atmospheric and Space Physics, 431 UCB, Colorado Center for Astrodynamics Research. Associate Fellow AIAA.

‡ADCS Integrated Simulation Software Lead, Laboratory for Atmospheric and Space Physics.

Note, Newtonian and Eulerian mechanics is the method chosen for the ease of compact vector notation, as well as the explicit forms of internal forces and torques that are produced [2,25]. However, note that the presented general spacecraft dynamics formulation is not tied to this method of deriving the equations of motion.

There is a need for a general solution to model the flexing behavior of spacecraft that can be readily implemented into software and be computationally efficient. This Note introduces a solution for modeling the flexible dynamics of the solar panels by assuming that the hub of the spacecraft and the solar panels are rigid bodies, but the solar panels are connected to the hub by single-degree-of-freedom torsional springs. This is a first-order approximation to the actual structural deflection phenomenon; but, for simulation and analysis purposes, this approximation is beneficial to computational speed and control system performance analysis. The torsional spring constants and damping coefficients can be attenuated to match the natural first-order frequencies of the solar panels found from finite element analysis or testing. An additional contribution of this work is a backsubstitution method to increase the computational efficiency and is similar to Ref. [25] for reaction wheels, but it is expanded to problems for which the translational and rotational motions are coupled. In addition to increasing the computational efficiency, the backsubstitution method aims to modularize the solution by oneway decoupling the equations, which will benefit a software implementation within a modular dynamics architecture.

II. Problem Statement

The purpose of this Note is to develop differential equations of motion describing a general spacecraft configuration with flexible appendage dynamics that can be readily integrated into a computer simulation. This avoids the need of deriving equations of motion for future spacecraft mission concepts. This formulation is developed in a general manner that applies to a wide range of spacecraft configurations and panel locations. The descriptions of the spacecraft, components, coordinate frames, and variables are introduced in Fig. 1.

The particular spacecraft in Fig. 1 is composed of a rigid-body hub connected to two solar panels by one-degree-of-freedom joints. These joints are modeled as torsional hinges with a linear spring constant of k_i and an angular rate damping term c_i. Two panels are shown for simplicity; however, the following formulation assumes there are N_s number of solar panels, each with a general location and hinge axis.

There are four coordinate frames defined for this formulation. The inertial reference frame is indicated by $\mathcal{N}$:$\{\hat{\boldsymbol{n}}_1, \hat{\boldsymbol{n}}_2, \hat{\boldsymbol{n}}_3\}$, and the dynamics are developed with respect to this reference frame. The body-fixed coordinate frame $\mathcal{B}$:$\{\hat{\boldsymbol{b}}_1, \hat{\boldsymbol{b}}_2, \hat{\boldsymbol{b}}_3\}$ is defined with its origin B, which can be located anywhere fixed to the hub; and the $\mathcal{B}$ frame can be oriented in any configuration. The ith solar panel frame $\mathcal{S}_i$:$\{\hat{\boldsymbol{s}}_{i,1}, \hat{\boldsymbol{s}}_{i,2}, \hat{\boldsymbol{s}}_{i,3}\}$ has its basis vectors oriented in the same direction because the principle axes of the solar panel and its origin are coincident with the ith hinge joint H_i. The $\mathcal{S}_i$ frame is oriented such that $\hat{\boldsymbol{s}}_{i,1}$ points antiparallel to the center of mass of the solar panel S_i, and the variable d_i defines the distance between points H_i and S_i. The $\hat{\boldsymbol{s}}_{i,2}$ axis is defined as the rotation axis that will yield a positive θ_i using the right-hand rule. The ith hinge frame $\mathcal{H}_i$:$\{\hat{\boldsymbol{h}}_{i,1}, \hat{\boldsymbol{h}}_{i,2}, \hat{\boldsymbol{h}}_{i,3}\}$ is a frame fixed with respect to the body frame, and it is equivalent to the respective $\mathcal{S}_i$ frame when the solar panel is undeflected. As can be seen in Fig. 1, $\hat{\boldsymbol{s}}_{i,2} = \hat{\boldsymbol{h}}_{i,2}$; therefore, θ_i defines a single-axis rotation of the $\mathcal{S}_i$ with respect to the $\mathcal{H}_i$ frame.

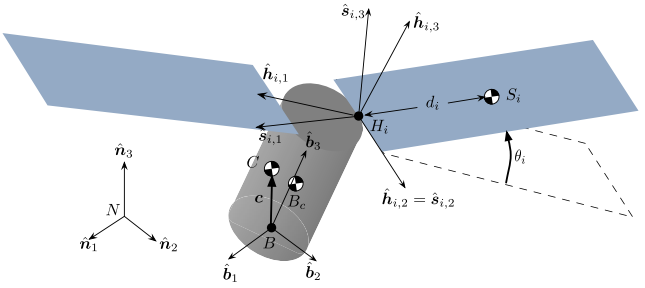

Fig. 1 Components, variables, and coordinate frames used for this derivation.

The location C is the center of mass location of the entire spacecraft, and B_c is the body-fixed center of mass location of the rigid-body hub. The vector $\boldsymbol{c}$ points from the origin of the body frame to the center of mass of the spacecraft. It is important to acknowledge that points B, B_c, and C are not necessarily coincident; and this assumption can be very useful when defining the spacecraft parameters. Simulation teams typically work very closely with structural engineering teams to define the spacecraft mass properties, and the general point B assumption gives much more flexibility in this technical interchange.

III. Derivation of Equations of Motion

Next, the equations of motion (EOMs) are derived using Newtonian and Eulerian mechanics. This approach allows for a general set of rigid hub attitude coordinates to be used while still describing the hub rotation rate through the convenient body angular velocity vector. Using Kane's method will also result in this decoupled form, but special identities and further algebra for simplification will be required to use Lagrangian mechanics. EOMs are required for the translational, rotational, and solar panel motion.

A. Spacecraft Translational Equations of Motion

The derivation of the hub translational equations of motion begins with Newton's second law for the center of mass of the spacecraft:

$$\boldsymbol{F}_{\text{ext}} = m_{\text{sc}}\ddot{\boldsymbol{r}}_{C/N} \tag{1}$$

where $\boldsymbol{r}_{C/N}$ defines the vector pointing from point N to point C, $\boldsymbol{F}_{\text{ext}}$ is the sum of the external forces acting on the spacecraft, and m_{sc} is the total mass of the spacecraft. Finding the hub EOM requires describing the acceleration of the origin of the body frame, point B

$$\ddot{\boldsymbol{r}}_{B/N} = \ddot{\boldsymbol{r}}_{C/N} - \ddot{\boldsymbol{c}} \tag{2}$$

where the center of mass vector $\boldsymbol{c}$ is

$$\boldsymbol{c} = \frac{m_{\text{hub}}\boldsymbol{r}_{B_c/B} + \sum_{i=1}^{N_s} m_{\text{sp}_i}\boldsymbol{r}_{S_i/B}}{m_{\text{sc}}} \tag{3}$$

where

$$m_{\text{sc}} = m_{\text{hub}} + \sum_{i=1}^{N_s} m_{\text{sp}_i}$$

is the total mass of the spacecraft.

To find the inertial time derivative of $\boldsymbol{c}$, it is first convenient to find the time derivative of $\boldsymbol{c}$ with respect to the body frame. A time derivative of a vector $\boldsymbol{v}$ with respect to the body frame $\mathcal{B}$ is denoted by $\boldsymbol{v}'$; the inertial time derivative is labeled as $\dot{\boldsymbol{v}}$.

The variable $\boldsymbol{r}_{S_i/H_i}$ is easily defined using the $\hat{\boldsymbol{s}}_{i,1}$ axis

$$\boldsymbol{r}_{S_i/H_i} = -d_i\hat{\boldsymbol{s}}_{i,1} \tag{4}$$

To find the body-frame-relative time derivative of $\boldsymbol{c}$, the first and second time derivatives with respect to the body frame of $\boldsymbol{r}_{S_i/H_i}$ are taken:

$$\boldsymbol{r}'_{S_i/H_i} = d_i\dot{\theta}_i\hat{\boldsymbol{s}}_{i,3} \qquad \boldsymbol{r}''_{S_i/H_i} = d_i(\ddot{\theta}_i\hat{\boldsymbol{s}}_{i,3} + \dot{\theta}_i^2\hat{\boldsymbol{s}}_{i,1}) \tag{5}$$

Referring to Eq. (3), taking the first and second body frame relative time derivatives of $\boldsymbol{c}$ yields

$$\boldsymbol{c}' = \frac{\sum_{i=1}^{N_s} m_{\text{sp}_i} d_i\dot{\theta}_i\hat{\boldsymbol{s}}_{i,3}}{m_{\text{sc}}} \qquad \boldsymbol{c}'' = \frac{\sum_{i=1}^{N_s} m_{\text{sp}_i} d_i(\ddot{\theta}_i\hat{\boldsymbol{s}}_{i,3} + \dot{\theta}_i^2\hat{\boldsymbol{s}}_{i,1})}{m_{\text{sc}}} \tag{6}$$

The transport theorem [25] maps the time derivative of vector $\boldsymbol{v}$ as seen by one frame $\mathcal{B}$ into the time derivative as seen by another frame $\mathcal{N}$ through

$$\dot{\boldsymbol{v}} = \boldsymbol{v}' + \boldsymbol{\omega}_{\mathcal{B}/\mathcal{N}} \times \boldsymbol{v} \tag{7}$$

Using the transport theorem, the inertial second derivative $\ddot{\boldsymbol{c}}$ is expressed in terms of body relative derivatives of $\boldsymbol{c}$ as

$$\ddot{\boldsymbol{c}} = \boldsymbol{c}'' + 2\boldsymbol{\omega}_{\mathcal{B}/\mathcal{N}} \times \boldsymbol{c}' + \dot{\boldsymbol{\omega}}_{\mathcal{B}/\mathcal{N}} \times \boldsymbol{c} + \boldsymbol{\omega}_{\mathcal{B}/\mathcal{N}} \times (\boldsymbol{\omega}_{\mathcal{B}/\mathcal{N}} \times \boldsymbol{c}) \tag{8}$$

where $\boldsymbol{\omega}_{\mathcal{B}/\mathcal{N}}$ is the angular velocity vector of frame $\mathcal{B}$ with respect to frame $\mathcal{N}$. Substituting Eq. (8) into the translational equations of motion in Eq. (2) results in

$$\ddot{\boldsymbol{r}}_{B/N} = \ddot{\boldsymbol{r}}_{C/N} - \boldsymbol{c}'' - 2\boldsymbol{\omega}_{\mathcal{B}/\mathcal{N}} \times \boldsymbol{c}' + \dot{\boldsymbol{\omega}}_{\mathcal{B}/\mathcal{N}} \times \boldsymbol{c} - \boldsymbol{\omega}_{\mathcal{B}/\mathcal{N}} \times (\boldsymbol{\omega}_{\mathcal{B}/\mathcal{N}} \times \boldsymbol{c}) \tag{9}$$

It is evident by looking at Eqs. (6) and (9) that the angular acceleration of the body $\dot{\boldsymbol{\omega}}_{\mathcal{B}/\mathcal{N}}$ and the angular acceleration of each solar panel angle $\ddot{\theta}_i$ are coupled with the translational acceleration $\ddot{\boldsymbol{r}}_{B/N}$. Because these are accelerations of state variables that will ultimately populate a system mass matrix, Eq. (9) is rearranged with the second-order state variable terms isolated on the left-hand side of the equation. The mass of the spacecraft m_{sc} is multiplied on both sides of the equation, which results in the substitution of the sum of the external forces applied on the spacecraft seen in Eq. (1):

$$\begin{aligned} m_{\text{sc}}\ddot{\boldsymbol{r}}_{B/N} - m_{\text{sc}}\boldsymbol{c} \times \dot{\boldsymbol{\omega}}_{\mathcal{B}/\mathcal{N}} + \sum_{i=1}^{N_s} m_{\text{sp}_i} d_i \hat{\boldsymbol{s}}_{i,3} \ddot{\theta}_i = \boldsymbol{F}_{\text{ext}} - 2m_{\text{sc}}\boldsymbol{\omega}_{\mathcal{B}/\mathcal{N}} \times \boldsymbol{c}' \\ - m_{\text{sc}}\boldsymbol{\omega}_{\mathcal{B}/\mathcal{N}} \times (\boldsymbol{\omega}_{\mathcal{B}/\mathcal{N}} \times \boldsymbol{c}) - \sum_{i=1}^{N_s} m_{\text{sp}_i} d_i \dot{\theta}_i^2 \hat{\boldsymbol{s}}_{i,1} \end{aligned} \tag{10}$$

This frame-independent vector equation describes the translational motion of body frame point B with respect to the inertial frame and is in terms of the rotational motion and solar panel motion.

B. Spacecraft Rotational Equations of Motion

Next, the EOM for the hub rotational motion is developed. The rigid-body rotational motion is most conveniently expressed by separating the kinematic and kinetic differential equations. This allows for any choice of attitude coordinates to be used to describe the orientation, whereas the convenient use of the quasi-velocity vector $\boldsymbol{\omega}_{B/N}$ is retained [25]. The kinetic rotational EOM derivation starts with Euler's equation when the body-fixed coordinate frame origin is not coincident with the center of mass of the body [25]:

$$\dot{\boldsymbol{H}}_{\text{sc},B} = \boldsymbol{L}_B + m_{\text{sc}}\ddot{\boldsymbol{r}}_{B/N} \times \boldsymbol{c} \tag{11}$$

Here, the vector $\boldsymbol{L}_B$ is the total external torque about point B. The definition of the angular momentum vector of the spacecraft about point B is as follows:

$$\begin{aligned} \boldsymbol{H}_{\text{sc},B} = [I_{\text{hub},B_c}]\boldsymbol{\omega}_{\mathcal{B}/\mathcal{N}} + m_{\text{hub}}\boldsymbol{r}_{B_c/B} \times \dot{\boldsymbol{r}}_{B_c/B} + \sum_{i=1}^{N_s} ([I_{\text{sp}_i,S_i}]\boldsymbol{\omega}_{\mathcal{B}/\mathcal{N}} \\ + \dot{\theta}_i I_{s_i,2}\hat{\boldsymbol{h}}_{i,2} + m_{\text{sp}_i}\boldsymbol{r}_{S_i/B} \times \dot{\boldsymbol{r}}_{S_i/B}) \end{aligned} \tag{12}$$

The solar panel frame $\mathcal{S}_i$ is assumed to be a principle frame such that the solar panel inertia matrix about its center of mass when defined with respect to the $\mathcal{S}_i$ frame is as follows:

$${}^{\mathcal{S}_i}[I_{\text{sp}_i,S_i}] = \begin{bmatrix} I_{s_{i,1}} & 0 & 0 \\ 0 & I_{s_{i,2}} & 0 \\ 0 & 0 & I_{s_{i,3}} \end{bmatrix} \tag{13}$$

The inertial time derivative of Eq. (12) is evaluated again using the transport theorem [25] to related vector derivatives as seen by different rotating frames and yields:

$$\begin{aligned} \dot{\boldsymbol{H}}_{\text{sc},B} = [I_{\text{hub},B_c}]\dot{\boldsymbol{\omega}}_{\mathcal{B}/\mathcal{N}} + \boldsymbol{\omega}_{\mathcal{B}/\mathcal{N}} \times [I_{\text{hub},B_c}]\boldsymbol{\omega}_{\mathcal{B}/\mathcal{N}} + m_{\text{hub}}\boldsymbol{r}_{B_c/B} \times \ddot{\boldsymbol{r}}_{B_c/B} \\ + \sum_{i=1}^{N_s} ([I'_{\text{sp}_i,S_i}]\boldsymbol{\omega}_{\mathcal{B}/\mathcal{N}} + [I_{\text{sp}_i,S_i}]\dot{\boldsymbol{\omega}}_{\mathcal{B}/\mathcal{N}} + \boldsymbol{\omega}_{\mathcal{B}/\mathcal{N}} \times [I_{\text{sp}_i,S_i}]\boldsymbol{\omega}_{\mathcal{B}/\mathcal{N}} \\ + \ddot{\theta}_i I_{s_i,2}\hat{\boldsymbol{h}}_{i,2} + \boldsymbol{\omega}_{\mathcal{B}/\mathcal{N}} \times \dot{\theta}_i I_{s_i,2}\hat{\boldsymbol{h}}_{i,2} + m_{\text{sp}_i}\boldsymbol{r}_{S_i/B} \times \ddot{\boldsymbol{r}}_{S_i/B}) \end{aligned} \tag{14}$$

The terms $\ddot{\boldsymbol{r}}_{B_c/B}$ and $\ddot{\boldsymbol{r}}_{S_i/B}$ are also found by using the transport theorem and taking advantage of $\boldsymbol{r}_{B_c/B}$ being fixed with respect to the body frame:

$$\ddot{\boldsymbol{r}}_{B_c/B} = \dot{\boldsymbol{\omega}}_{\mathcal{B}/\mathcal{N}} \times \boldsymbol{r}_{B_c/B} + \boldsymbol{\omega}_{\mathcal{B}/\mathcal{N}} \times (\boldsymbol{\omega}_{\mathcal{B}/\mathcal{N}} \times \boldsymbol{r}_{B_c/B}) \tag{15}$$

$$\begin{aligned} \ddot{\boldsymbol{r}}_{S_i/B} = \boldsymbol{r}''_{S_i/B} + 2\boldsymbol{\omega}_{\mathcal{B}/\mathcal{N}} \times \boldsymbol{r}'_{S_i/B} + \dot{\boldsymbol{\omega}}_{\mathcal{B}/\mathcal{N}} \times \boldsymbol{r}_{S_i/B} + \boldsymbol{\omega}_{\mathcal{B}/\mathcal{N}} \\ \times (\boldsymbol{\omega}_{\mathcal{B}/\mathcal{N}} \times \boldsymbol{r}_{S_i/B}) \end{aligned} \tag{16}$$

Incorporating Eqs. (15) and (16) into Eq. (14) and simplifying the extensive algebra results in the intermediate result,

$$\begin{aligned} \dot{\boldsymbol{H}}_{\text{sc},B} = \left[I_{\text{hub},B_c}\right]\dot{\boldsymbol{\omega}}_{\mathcal{B}/\mathcal{N}} + \boldsymbol{\omega}_{\mathcal{B}/\mathcal{N}} \times \left[I_{\text{hub},B_c}\right]\boldsymbol{\omega}_{\mathcal{B}/\mathcal{N}} + m_{\text{hub}}\boldsymbol{r}_{B_c/B} \\ \times \left(\dot{\boldsymbol{\omega}}_{\mathcal{B}/\mathcal{N}} \times \boldsymbol{r}_{B_c/B}\right) + m_{\text{hub}}\boldsymbol{r}_{B_c/B} \times \left[\boldsymbol{\omega}_{\mathcal{B}/\mathcal{N}} \times \left(\boldsymbol{\omega}_{\mathcal{B}/\mathcal{N}} \times \boldsymbol{r}_{B_c/B}\right)\right] \\ + \sum_{i=1}^{N_s} \Big(\left[I'_{\text{sp}_i,S_i}\right]\boldsymbol{\omega}_{\mathcal{B}/\mathcal{N}} + \left[I_{\text{sp}_i,S_i}\right]\dot{\boldsymbol{\omega}}_{\mathcal{B}/\mathcal{N}} + \boldsymbol{\omega}_{\mathcal{B}/\mathcal{N}} \times \left[I_{\text{sp}_i,S_i}\right]\boldsymbol{\omega}_{\mathcal{B}/\mathcal{N}} \\ + \ddot{\theta}_i I_{s_i,2}\hat{\boldsymbol{h}}_{i,2} + \boldsymbol{\omega}_{\mathcal{B}/\mathcal{N}} \times \dot{\theta}_i I_{s_i,2}\hat{\boldsymbol{h}}_{i,2} + m_{\text{sp}_i}\boldsymbol{r}_{S_i/B} \times \boldsymbol{r}''_{S_i/B} \\ + 2m_{\text{sp}_i}\boldsymbol{r}_{S_i/B} \times \left(\boldsymbol{\omega}_{\mathcal{B}/\mathcal{N}} \times \boldsymbol{r}'_{S_i/B}\right) + m_{\text{sp}_i}\boldsymbol{r}_{S_i/B} \times \left(\dot{\boldsymbol{\omega}}_{\mathcal{B}/\mathcal{N}} \times \boldsymbol{r}_{S_i/B}\right) \\ + m_{\text{sp}_i}\boldsymbol{r}_{S_i/B} \times \left[\boldsymbol{\omega}_{\mathcal{B}/\mathcal{N}} \times \left(\boldsymbol{\omega}_{\mathcal{B}/\mathcal{N}} \times \boldsymbol{r}_{S_i/B}\right)\right] \Big) \end{aligned} \tag{17}$$

Using the inertia matrix parallel axis theorem [25], some simplified inertia matrix terms are defined in Eqs. (18–21). These equations use the skew-symmetric matrix definition: $\boldsymbol{a} \times \boldsymbol{b}$ is the crossproduct between $\boldsymbol{a}$ and $\boldsymbol{b}$ as a vector equation and can be expressed in matrix form as $[\tilde{\boldsymbol{a}}]\boldsymbol{b}$, where $[\tilde{\boldsymbol{a}}]$ is a 3×3 matrix, $\boldsymbol{b}$ is a 3×1 matrix, and their components are expressed with respect to the same frame [25]. Equations (18–24) are matrix equations and the reference frame is not specified to keep the formulation frame independent. It is assumed that when evaluating Eqs. (18–24) the matrices are all defined with respect to the same reference frame.

$$[I_{\text{hub},B}] = [I_{\text{hub},B_c}] + m_{\text{hub}}[\tilde{\boldsymbol{r}}_{B_c/B}][\tilde{\boldsymbol{r}}_{B_c/B}]^T \tag{18}$$

$$[I_{\text{sp}_i,B}] = [I_{\text{sp}_i,S_i}] + m_{\text{sp}_i}[\tilde{\boldsymbol{r}}_{S_i/B}][\tilde{\boldsymbol{r}}_{S_i/B}]^T \tag{19}$$

$$[I_{\text{sc},B}] = [I_{\text{hub},B}] + \sum_{i}^{P} [I_{\text{sp}_i,B}] \tag{20}$$

$$[I'_{\text{sc},B}] = \sum_{i=1}^{N_s} [[I'_{\text{sp}_i,S_i}] - m_{\text{sp}_i}([\tilde{\boldsymbol{r}}'_{S_i/B}][\tilde{\boldsymbol{r}}_{S_i/B}] + [\tilde{\boldsymbol{r}}_{S_i/B}][\tilde{\boldsymbol{r}}'_{S_i/B}])] \tag{21}$$

$[I'_{\text{sp}_i,S_i}]$ needs to be defined and is conveniently expressed by leveraging the assumption that the inertia matrix is diagonal and can be written in terms of its base vectors:

$$[I_{\text{sp}_i,S_i}] = I_{s_{i,1}}\hat{\boldsymbol{s}}_{i,1}\hat{\boldsymbol{s}}_{i,1}^T + I_{s_{i,2}}\hat{\boldsymbol{s}}_{i,2}\hat{\boldsymbol{s}}_{i,2}^T + I_{s_{i,3}}\hat{\boldsymbol{s}}_{i,3}\hat{\boldsymbol{s}}_{i,3}^T \tag{22}$$

Equation (22) is a matrix equation using the notation that $\boldsymbol{a}\boldsymbol{b}^T$ is the outer product between two 3×1 matrices. Again, this equation is

assumed to be expressed with respect to one specific frame. Taking the body relative time derivative of Eq. (22) results in

$$[I'_{\mathrm{sp}_i,\mathcal{S}_i}] = I_{s_{i,1}}\hat{\boldsymbol{s}}'_{i,1}\hat{\boldsymbol{s}}^T_{i,1} + I_{s_{i,1}}\hat{\boldsymbol{s}}_{i,1}\hat{\boldsymbol{s}}'^T_{i,1} + I_{s_{i,2}}\hat{\boldsymbol{s}}'_{i,2}\hat{\boldsymbol{s}}^T_{i,2} + I_{s_{i,2}}\hat{\boldsymbol{s}}_{i,2}\hat{\boldsymbol{s}}'^T_{i,2} + I_{s_{i,3}}\hat{\boldsymbol{s}}'_{i,3}\hat{\boldsymbol{s}}^T_{i,3} + I_{s_{i,3}}\hat{\boldsymbol{s}}_{i,3}\hat{\boldsymbol{s}}'^T_{i,3} \tag{23}$$

Performing the $\mathcal{B}$-frame relative time derivatives and simplifying results in the following body-relative time derivative expression of the solar panel inertia matrix:

$$[I'_{\mathrm{sp}_i,\mathcal{S}_i}] = \dot{\theta}_i(I_{s_{i,3}} - I_{s_{i,1}})(\hat{\boldsymbol{s}}_{i,1}\hat{\boldsymbol{s}}^T_{i,3} + \hat{\boldsymbol{s}}_{i,3}\hat{\boldsymbol{s}}^T_{i,1}) \tag{24}$$

Using these definitions greatly simplifies the expression in Eq. (17), yielding the compact expression

$$\begin{aligned}\dot{\boldsymbol{H}}_{\mathrm{sc},B} &= [I_{\mathrm{sc},B}]\dot{\boldsymbol{\omega}}_{\mathcal{B}/\mathcal{N}} + \boldsymbol{\omega}_{\mathcal{B}/\mathcal{N}} \times [I_{\mathrm{sc},B}]\boldsymbol{\omega}_{\mathcal{B}/\mathcal{N}} + [I'_{\mathrm{sc},B}]\boldsymbol{\omega}_{\mathcal{B}/\mathcal{N}} \\ &+ \sum_{i=1}^{N_s}\{\ddot{\theta}_i I_{s_i,2}\hat{\boldsymbol{h}}_{i,2} + \boldsymbol{\omega}_{\mathcal{B}/\mathcal{N}} \times \dot{\theta}_i I_{s_i,2}\hat{\boldsymbol{h}}_{i,2} + m_{\mathrm{sp}_i}\boldsymbol{r}_{S_i/B} \times \boldsymbol{r}''_{S_i/B} \\ &+ m_{\mathrm{sp}_i}\boldsymbol{\omega}_{\mathcal{B}/\mathcal{N}} \times (\boldsymbol{r}_{S_i/B} \times \boldsymbol{r}'_{S_i/B})\}\end{aligned} \tag{25}$$

Finally, Eqs. (11) and (25) are equated and all second-order state derivatives are moved to the left-hand side:

$$\begin{aligned}&m_{\mathrm{sc}}\boldsymbol{c} \times \ddot{\boldsymbol{r}}_{B/N} + [I_{\mathrm{sc},B}]\dot{\boldsymbol{\omega}}_{\mathcal{B}/\mathcal{N}} + \sum_{i=1}^{N_s}\{I_{s_i,2}\hat{\boldsymbol{h}}_{i,2} + m_{\mathrm{sp}_i}d_i\boldsymbol{r}_{S_i/B} \times \hat{\boldsymbol{s}}_{i,3}\}\ddot{\theta}_i \\ &= -\boldsymbol{\omega}_{\mathcal{B}/\mathcal{N}} \times [I_{\mathrm{sc},B}]\boldsymbol{\omega}_{\mathcal{B}/\mathcal{N}} - [I'_{\mathrm{sc},B}]\boldsymbol{\omega}_{\mathcal{B}/\mathcal{N}} - \sum_{i=1}^{N_s}\{\dot{\theta}_i\boldsymbol{\omega}_{\mathcal{B}/\mathcal{N}} \\ &\times (I_{s_i,2}\hat{\boldsymbol{h}}_{i,2} + m_{\mathrm{sp}_i}d_i\boldsymbol{r}_{S_i/B} \times \hat{\boldsymbol{s}}_{i,3}) + m_{\mathrm{sp}_i}d_i\dot{\theta}_i^2\boldsymbol{r}_{S_i/B} \times \hat{\boldsymbol{s}}_{i,1}\} + \boldsymbol{L}_B\end{aligned} \tag{26}$$

This expanded rotational equation of motion for a rigid hub with N_s hinged panels shows the additional terms required to account for the multi-body interaction between the rigid-body hub and the deflecting hinged panels.

C. Hinged Panel Equations of Motion

The set of EOMs required to solve this system of differential equations is related to the hinged rigid panels, which can represent solar panel flexing. In this development, the ith solar panel frame $\mathcal{S}_i$ is assumed to be a principal coordinate frame of the panel, yielding the diagonal inertia matrix representation shown in Eq. (13).

Let

$$\boldsymbol{L}_{H_i} = L_{i,1}\hat{\boldsymbol{s}}_{i,1} + L_{i,2}\hat{\boldsymbol{s}}_{i,2} + L_{i,3}\hat{\boldsymbol{s}}_{i,3}$$

be the total torque acting on the solar panel about the hinge point H_i. The corresponding hinge torque component about the body-fixed hinge axis $\hat{\boldsymbol{s}}_{i,2}$ is given through

$$L_{i,2} = -k_i\theta_i - c_i\dot{\theta}_i + \hat{\boldsymbol{s}}_{i,2} \cdot \boldsymbol{\tau}_{\mathrm{ext},H_i} \tag{27}$$

The hinge structure produces the other two torques $L_{i,1}$ and $L_{i,3}$. The vector $\boldsymbol{\tau}_{\mathrm{ext},H_i}$ is the net external torque on the solar panel and is projected onto the $\hat{\boldsymbol{s}}_{i,2}$ direction to find its contribution to $L_{i,2}$. Gravity, for example, will apply the following torque on the solar panel about point H_i: $\boldsymbol{\tau}_{g,H_i} = \boldsymbol{r}_{S_i/H_i} \times \boldsymbol{F}_g$.

The inertial angular velocity vector for the solar panel frame is

$$\boldsymbol{\omega}_{\mathcal{S}_i/\mathcal{N}} = \boldsymbol{\omega}_{\mathcal{S}_i/\mathcal{H}_i} + \boldsymbol{\omega}_{\mathcal{H}_i/\mathcal{B}} + \boldsymbol{\omega}_{\mathcal{B}/\mathcal{N}} \tag{28}$$

where $\boldsymbol{\omega}_{\mathcal{S}_i/\mathcal{H}_i} = \dot{\theta}_i\hat{\boldsymbol{s}}_{i,2}$. Because the hinge frame $\mathcal{H}_i$ is fixed relative to the body frame $\mathcal{B}$, the relative angular velocity vector is $\boldsymbol{\omega}_{\mathcal{H}_i/\mathcal{B}} = \boldsymbol{0}$. The body angular velocity vector is written in the $\mathcal{S}_i$-frame components as

$$\begin{aligned}\boldsymbol{\omega}_{\mathcal{B}/\mathcal{N}} &= (\hat{\boldsymbol{s}}_{i,1} \cdot \boldsymbol{\omega}_{\mathcal{B}/\mathcal{N}})\hat{\boldsymbol{s}}_{i,1} + (\hat{\boldsymbol{s}}_{i,2} \cdot \boldsymbol{\omega}_{\mathcal{B}/\mathcal{N}})\hat{\boldsymbol{s}}_{i,2} + (\hat{\boldsymbol{s}}_{i,3} \cdot \boldsymbol{\omega}_{\mathcal{B}/\mathcal{N}})\hat{\boldsymbol{s}}_{i,3} \\ &= \omega_{s_{i,1}}\hat{\boldsymbol{s}}_{i,1} + \omega_{s_{i,2}}\hat{\boldsymbol{s}}_{i,2} + \omega_{s_{i,3}}\hat{\boldsymbol{s}}_{i,3}\end{aligned} \tag{29}$$

Fortunately, using this definition greatly simplifies the following algebraic development. Finally, the inertial solar panel angular velocity vector is written as

$$\boldsymbol{\omega}_{\mathcal{S}_i/\mathcal{N}} = \omega_{s_{i,1}}\hat{\boldsymbol{s}}_{i,1} + (\omega_{s_{i,2}} + \dot{\theta}_i)\hat{\boldsymbol{s}}_{i,2} + \omega_{s_{i,3}}\hat{\boldsymbol{s}}_{i,3} \tag{30}$$

Substituting these angular velocity components into the rotational equations of motion of a rigid body with torques taken about its center of mass [25], the general solar panel equations of motion are written as

$$I_{s_{i,1}}\dot{\omega}_{s_{i,1}} = -(I_{s_{i,3}} - I_{s_{i,2}})(\omega_{s_{i,2}} + \dot{\theta}_i)\omega_{s_{i,3}} + L_{s_{i,1}} \tag{31}$$

$$I_{s_{i,2}}(\dot{\omega}_{s_{i,2}} + \ddot{\theta}_i) = -(I_{s_{i,1}} - I_{s_{i,3}})\omega_{s_{i,3}}\omega_{s_{i,1}} + L_{s_{i,2}} \tag{32}$$

$$I_{s_{i,3}}\dot{\omega}_{s_{i,3}} = -(I_{s_{i,2}} - I_{s_{i,1}})\omega_{s_{i,1}}(\omega_{s_{i,2}} + \dot{\theta}_i) + L_{s_{i,3}} \tag{33}$$

where

$$\boldsymbol{L}_{S_i} = L_{s_{i,1}}\hat{\boldsymbol{s}}_{i,1} + L_{s_{i,2}}\hat{\boldsymbol{s}}_{i,2} + L_{s_{i,3}}\hat{\boldsymbol{s}}_{i,3}$$

is the net torque acting on the solar panel about its center of mass. Note that the second differential equation in Eq. (32) is used to get the desired equations of motion of θ_i. The first and third equations could be used to backsolve for the structural hinge torques embedded in $L_{s_{i,1}}$ and $L_{s_{i,3}}$ if needed.

The torque about the solar panel center of mass can be related to the torque about the hinge point H_i using

$$\boldsymbol{L}_{S_i} = \boldsymbol{L}_{H_i} - r_{S_i/H_i} \times m_{\mathrm{sp}_i}\ddot{\boldsymbol{r}}_{S_i/N} \tag{34}$$

Taking the vector dot product of Eq. (34) with $\hat{\boldsymbol{s}}_{i,2}$ and using $\boldsymbol{r}_{S_i/H_i} = -d_i\hat{\boldsymbol{s}}_{i,1}$ allows for a scalar equation to be developed that relates the hinge axis torque $\boldsymbol{L}_{s_{i,2}}$:

$$\begin{aligned}L_{s_{i,2}} &= \hat{\boldsymbol{s}}_{i,2} \cdot \boldsymbol{L}_{S_i} = \hat{\boldsymbol{s}}_{i,2} \cdot \boldsymbol{L}_{H_i} - \hat{\boldsymbol{s}}_{i,2} \cdot (\boldsymbol{r}_{S_i/H_i} \times m_{\mathrm{sp}_i}\ddot{\boldsymbol{r}}_{S_i/N}) \\ &= -k_i\theta - c_i\dot{\theta}_i + \hat{\boldsymbol{s}}_{i,2} \cdot \boldsymbol{\tau}_{\mathrm{ext},H_i} + m_{\mathrm{sp}_i}d_i\hat{\boldsymbol{s}}_{i,2} \cdot (\hat{\boldsymbol{s}}_{i,1} \times \ddot{\boldsymbol{r}}_{S_i/N})\end{aligned} \tag{35}$$

Solving for the second-order inertial time derivative of $\boldsymbol{r}_{S_i/N} = \boldsymbol{r}_{H_i/N} - d\hat{\boldsymbol{s}}_{i,1}$ yields

$$\ddot{\boldsymbol{r}}_{S_i/N} = \ddot{\boldsymbol{r}}_{H_i/N} - \dot{\boldsymbol{\omega}}_{\mathcal{S}_i/\mathcal{N}} \times (d\hat{\boldsymbol{s}}_{i,1}) - \boldsymbol{\omega}_{\mathcal{S}_i/\mathcal{N}} \times (\boldsymbol{\omega}_{\mathcal{S}_i/\mathcal{N}} \times (d\hat{\boldsymbol{s}}_{i,1})) \tag{36}$$

Substituting this inertial acceleration into the preceding $L_{s_{i,2}}$ and simplifying using the double vector crossproduct identity, as well as $\boldsymbol{a} \cdot (\boldsymbol{b} \times \boldsymbol{c}) = (\boldsymbol{a} \times \boldsymbol{b}) \cdot \boldsymbol{c}$, $L_{s_{i,2}}$ yields

$$\begin{aligned}L_{s_{i,2}} &= -k_i\theta_i - c_i\dot{\theta}_i + \hat{\boldsymbol{s}}_{i,2} \cdot \boldsymbol{\tau}_{\mathrm{ext},H_i} - m_{\mathrm{sp}_i}d_i\hat{\boldsymbol{s}}_{i,3} \cdot \ddot{\boldsymbol{r}}_{H_i/N} - m_{\mathrm{sp}_i}d_i^2\hat{\boldsymbol{s}}_{i,2} \\ &\cdot \dot{\boldsymbol{\omega}}_{\mathcal{B}/\mathcal{N}} - m_{\mathrm{sp}_i}d_i^2\ddot{\theta}_i + m_{\mathrm{sp}_i}d_i^2\omega_{s_{i,3}}\omega_{s_{i,1}}\end{aligned} \tag{37}$$

Substituting this torque into the differential equation seen in Eq. (33) yields the desired scalar hinged solar panel equation of motion:

$$\begin{aligned}&(I_{s_{i,2}} + m_{\mathrm{sp}_i}d_i^2)\hat{\boldsymbol{s}}_{i,2} \cdot \dot{\boldsymbol{\omega}}_{\mathcal{B}/\mathcal{N}} + (I_{s_{i,2}} + m_{\mathrm{sp}_i}d_i^2)\ddot{\theta}_i + m_{\mathrm{sp}_i}d_i\hat{\boldsymbol{s}}_{i,3} \cdot \ddot{\boldsymbol{r}}_{H_i/N} \\ &+ k_i\theta + c_i\dot{\theta}_i - \hat{\boldsymbol{s}}_{i,2} \cdot \boldsymbol{\tau}_{\mathrm{ext},H_i} + (I_{s_{i,1}} - I_{s_{i,3}} - m_{\mathrm{sp}_i}d_i^2)\omega_{s_{i,3}}\omega_{s_{i,1}} = 0\end{aligned} \tag{38}$$

The final task is to expand $\ddot{\boldsymbol{r}}_{H_i/N}$ in terms of the translational motion $\ddot{\boldsymbol{r}}_{B/N}$, recalling that the hinge location is a fixed point on

the body. The final expression again groups the second-order state variables conveniently to the left-hand side of the equation:

$$m_{\mathrm{sp}_i} d_i \hat{\boldsymbol{s}}_{i,3} \cdot \ddot{\boldsymbol{r}}_{B/N} + (I_{s_{i,2}} + m_{\mathrm{sp}_i} d_i^2)\hat{s}_{i,2} \cdot \dot{\boldsymbol{\omega}}_{\mathcal{B}/\mathcal{N}} - m_{\mathrm{sp}_i} d_i \hat{\boldsymbol{s}}_{i,3} \cdot (\boldsymbol{r}_{H_i/B} \times \dot{\boldsymbol{\omega}}_{\mathcal{B}/\mathcal{N}}) + (I_{s_{i,2}} + m_{\mathrm{sp}_i} d_i^2)\ddot{\theta}_i = -k_i\theta_i - c_i\dot{\theta}_i + \hat{\boldsymbol{s}}_{i,2} \cdot \boldsymbol{\tau}_{\mathrm{ext},H_i} + (I_{s_{i,3}} - I_{s_{i,1}} + m_{\mathrm{sp}_i} d_i^2)\omega_{s_{i,3}}\omega_{s_{i,1}} - m_{\mathrm{sp}_i} d_i \hat{\boldsymbol{s}}_{i,3} \cdot [\boldsymbol{\omega}_{\mathcal{B}/\mathcal{N}} \times (\boldsymbol{\omega}_{\mathcal{B}/\mathcal{N}} \times \boldsymbol{r}_{H_i/B})] \tag{39}$$

Equation (39) provides the N_s scalar hinged panel EOMs required to describe the motion of the spacecraft.

IV. Backsubstitution Formulation

The equations presented in the previous sections result in $N_s + 6$ coupled kinetic differential equations. Note that the various kinematic differential equation for hub motion and rotation, as well as the flexing angles, are already decoupled in this formulation. Therefore, if the remaining $N + 6$ kinetic EOMs are placed into state space form, a system mass matrix with a size of $N_s + 6$ will need to be inverted to numerically integrate the dynamical system. This can result in a computationally expensive simulation for a large number of panels. In the following developments, the EOMs are manipulated using a backsubstitution method to yield a more modular EOM framework that is also faster to evaluate. This process is similar to how the reaction wheel EOMs are solved in Ref. [25]; however, this analytical backsubstitution is expanded to account for the coupled translational and rotational motions.

This section of the Note expresses the vector equations developed in the past section as matrix equations. These equations do not specify a reference frame to keep the formulation frame independent. However, when implementing these equations in software, all of the matrices need to be defined with respect to the same reference frame. A common frame in which to express the equations would be the body frame $\mathcal{B}$. Because these equations are matrix equations, the following notation will be used: $\boldsymbol{a} \times \boldsymbol{b}$ is expressed as $[\tilde{\boldsymbol{a}}]\boldsymbol{b}$, $\boldsymbol{a} \cdot \boldsymbol{b}$ is expressed as $\boldsymbol{a}^T\boldsymbol{b}$, and the outer products are expressed as $\boldsymbol{a}\boldsymbol{b}^T$.

A. Solar Panel Motion Manipulation

In Eq. (39), the solar panel motion is coupled with both the translational motion and the rotational motion. In addition, both the translational and rotational EOMs include the solar panel accelerations. To decouple the hub acceleration vectors from the panel accelerations, Eq. (39) is solved for the angular accelerations $\ddot{\theta}_i$:

$$\ddot{\theta}_i = \frac{1}{(I_{s_{i,2}} + m_{\mathrm{sp}_i} d_i^2)}(-m_{\mathrm{sp}_i} d_i \hat{\boldsymbol{s}}_{i,3}^T \ddot{\boldsymbol{r}}_{B/N} - [(I_{s_{i,2}} + m_{\mathrm{sp}_i} d_i^2)\hat{\boldsymbol{s}}_{i,2}^T - m_{\mathrm{sp}_i} d_i \hat{\boldsymbol{s}}_{i,3}^T[\tilde{\boldsymbol{r}}_{H_i/B}]]\dot{\boldsymbol{\omega}}_{\mathcal{B}/\mathcal{N}} - k_i\theta_i - c_i\dot{\theta}_i + \hat{\boldsymbol{s}}_{i,2}^T\boldsymbol{\tau}_{\mathrm{ext},H_i} + (I_{s_{i,3}} - I_{s_{i,1}} + m_{\mathrm{sp}_i} d_i^2)\omega_{s_{i,3}}\omega_{s_{i,1}} - m_{\mathrm{sp}_i} d_i \hat{\boldsymbol{s}}_{i,3}^T[\tilde{\boldsymbol{\omega}}_{\mathcal{B}/\mathcal{N}}][\tilde{\boldsymbol{\omega}}_{\mathcal{B}/\mathcal{N}}]\boldsymbol{r}_{H_i/B}) \tag{40}$$

Equation (40) is rewritten into the following compact form and will be used multiple times throughout this formulation:

$$\ddot{\theta}_i = \boldsymbol{a}_{\theta_i}^T \ddot{\boldsymbol{r}}_{B/N} + \boldsymbol{b}_{\theta_i}^T \dot{\boldsymbol{\omega}}_{\mathcal{B}/\mathcal{N}} + c_{\theta_i} \tag{41}$$

where $\boldsymbol{a}_{\theta_i}$, $\boldsymbol{b}_{\theta_i}$, and c_{θ_i} are defined in Eqs. (42–44):

$$\boldsymbol{a}_{\theta_i} = -\frac{m_{\mathrm{sp}_i} d_i}{\left(I_{s_{i,2}} + m_{\mathrm{sp}_i} d_i^2\right)} \hat{\boldsymbol{s}}_{i,3} \tag{42}$$

$$\boldsymbol{b}_{\theta_i} = -\frac{1}{\left(I_{s_{i,2}} + m_{\mathrm{sp}_i} d_i^2\right)}[(I_{s_{i,2}} + m_{\mathrm{sp}_i} d_i^2)\hat{\boldsymbol{s}}_{i,2} + m_{\mathrm{sp}_i} d_i[\tilde{\boldsymbol{r}}_{H_i/B}]\hat{\boldsymbol{s}}_{i,3}] \tag{43}$$

$$c_{\theta_i} = \frac{1}{(I_{s_{i,2}} + m_{\mathrm{sp}_i} d_i^2)}(-k_i\theta_i - c_i\dot{\theta}_i + \hat{\boldsymbol{s}}_{i,2} \cdot \boldsymbol{\tau}_{\mathrm{ext},H_i} + (I_{s_{i,3}} - I_{s_{i,1}} + m_{\mathrm{sp}_i} d_i^2)\omega_{s_{i,3}}\omega_{s_{i,1}} - m_{\mathrm{sp}_i} d_i \hat{\boldsymbol{s}}_{i,3}^T[\tilde{\boldsymbol{\omega}}_{\mathcal{B}/\mathcal{N}}] \times [\tilde{\boldsymbol{\omega}}_{\mathcal{B}/\mathcal{N}}]\boldsymbol{r}_{H_i/B}) \tag{44}$$

B. Decoupled Translational and Rotational Accelerations

To solve for the translational and rotational accelerations, Eq. (41) is substituted into the translational and rotational EOMs. The result of this substitution for the translation EOM [Eq. (10)] is seen in the following equation:

$$m_{\mathrm{sc}}\ddot{\boldsymbol{r}}_{B/N} - m_{\mathrm{sc}}[\tilde{\boldsymbol{c}}]\dot{\boldsymbol{\omega}}_{\mathcal{B}/\mathcal{N}} + \sum_{i=1}^{N_s} m_{\mathrm{sp}_i} d_i \hat{\boldsymbol{s}}_{i,3}(\boldsymbol{a}_{\theta_i}^T \ddot{\boldsymbol{r}}_{B/N} + \boldsymbol{b}_{\theta_i}^T \dot{\boldsymbol{\omega}}_{\mathcal{B}/\mathcal{N}} + c_{\theta_i}) = F_{\mathrm{ext}} - 2m_{\mathrm{sc}}[\tilde{\boldsymbol{\omega}}_{\mathcal{B}/\mathcal{N}}]\boldsymbol{c}' - m_{\mathrm{sc}}[\tilde{\boldsymbol{\omega}}_{\mathcal{B}/\mathcal{N}}][\tilde{\boldsymbol{\omega}}_{\mathcal{B}/\mathcal{N}}]\boldsymbol{c} - \sum_{i=1}^{N_s} m_{\mathrm{sp}_i} d_i \dot{\theta}_i^2 \hat{\boldsymbol{s}}_{i,1} \tag{45}$$

Simplifying and combining like terms yields the translational EOM that has been decoupled from the solar panel acceleration:

$$(m_{\mathrm{sc}}[\boldsymbol{I}_{3\times3}] + \sum_{i=1}^{N} m_{\mathrm{sp}_i} d_i \hat{\boldsymbol{s}}_{i,3}\boldsymbol{a}_{\theta_i}^T)\ddot{\boldsymbol{r}}_{B/N} + \left(-m_{\mathrm{sc}}[\tilde{\boldsymbol{c}}] + \sum_{i=1}^{N} m_{\mathrm{sp}_i} d_i \hat{\boldsymbol{s}}_{i,3}\boldsymbol{b}_{\theta_i}^T\right)\dot{\boldsymbol{\omega}}_{\mathcal{B}/\mathcal{N}} = m_{\mathrm{sc}}\ddot{\boldsymbol{r}}_{C/N} - 2m_{\mathrm{sc}}[\tilde{\boldsymbol{\omega}}_{\mathcal{B}/\mathcal{N}}]\boldsymbol{c}' - m_{\mathrm{sc}}[\tilde{\boldsymbol{\omega}}_{\mathcal{B}/\mathcal{N}}][\tilde{\boldsymbol{\omega}}_{\mathcal{B}/\mathcal{N}}]\boldsymbol{c} - \sum_{i=1}^{N}(m_{\mathrm{sp}_i} d_i \dot{\theta}_i^2 \hat{\boldsymbol{s}}_{i,1} + m_{\mathrm{sp}_i} d_i c_{\theta_i} \hat{\boldsymbol{s}}_{i,3}) \tag{46}$$

Following the same pattern for the rotational hub EOM [Eq. (26)] yields the following:

$$\left[m_{\mathrm{sc}}[\tilde{\boldsymbol{c}}] + \sum_{i=1}^{N}(I_{s_{i,2}}\hat{\boldsymbol{s}}_{i,2} + m_{\mathrm{sp}_i} d_i[\tilde{\boldsymbol{r}}_{S_{c,i}/B}]\hat{\boldsymbol{s}}_{i,3})\boldsymbol{a}_{\theta_i}^T\right]\ddot{\boldsymbol{r}}_{B/N} + \left[[I_{\mathrm{sc},B}] + \sum_{i=1}^{N}(I_{s_{i,2}}\hat{\boldsymbol{s}}_{i,2} + m_{\mathrm{sp}_i} d_i[\tilde{\boldsymbol{r}}_{S_{c,i}/B}]\hat{\boldsymbol{s}}_{i,3})\boldsymbol{b}_{\theta_i}^T\right]\dot{\boldsymbol{\omega}}_{\mathcal{B}/\mathcal{N}} = -[\tilde{\boldsymbol{\omega}}_{\mathcal{B}/\mathcal{N}}][I_{\mathrm{sc},B}]\boldsymbol{\omega}_{\mathcal{B}/\mathcal{N}} - [I'_{\mathrm{sc},B}]\boldsymbol{\omega}_{\mathcal{B}/\mathcal{N}} - \sum_{i=1}^{N}\{(\dot{\theta}_i[\tilde{\boldsymbol{\omega}}_{\mathcal{B}/\mathcal{N}}] + c_{\theta_i}[I_{3\times3}])(I_{s_{i,2}}\hat{\boldsymbol{s}}_{i,2} + m_{\mathrm{sp}_i} d_i[\tilde{\boldsymbol{r}}_{S_{c,i}/B}]\hat{\boldsymbol{s}}_{i,3}) + m_{\mathrm{sp}_i} d_i \dot{\theta}_i^2[\tilde{\boldsymbol{r}}_{S_{c,i}/B}]\hat{\boldsymbol{s}}_{i,1}\} + \boldsymbol{L}_B \tag{47}$$

The coupled translation and rotation hub EOMs can be written compactly as

$$\begin{bmatrix}[A] & [B]\\ [C] & [D]\end{bmatrix}\begin{bmatrix}\ddot{\boldsymbol{r}}_{B/N}\\ \dot{\boldsymbol{\omega}}_{\mathcal{B}/\mathcal{N}}\end{bmatrix} = \begin{bmatrix}\boldsymbol{v}_{\mathrm{trans}}\\ \boldsymbol{v}_{\mathrm{rot}}\end{bmatrix} \tag{48}$$

using the following matrices to yield the compact form:

$$[A] = m_{\mathrm{sc}}[I_{3\times3}] + \sum_{i=1}^{N} m_{\mathrm{sp}_i} d_i \hat{\boldsymbol{s}}_{i,3}\boldsymbol{a}_{\theta_i}^T$$

$$[B] = -m_{\mathrm{sc}}[\tilde{\boldsymbol{c}}] + \sum_{i=1}^{N} m_{\mathrm{sp}_i} d_i \hat{\boldsymbol{s}}_{i,3}\boldsymbol{b}_{\theta_i}^T \tag{49}$$

$$[C] = m_{\mathrm{sc}}[\tilde{\boldsymbol{c}}] + \sum_{i=1}^{N}(I_{s_{i,2}}\hat{\boldsymbol{s}}_{i,2} + m_{\mathrm{sp}_i} d_i[\tilde{\boldsymbol{r}}_{S_{c,i}/B}]\hat{\boldsymbol{s}}_{i,3})\boldsymbol{a}_{\theta_i}^T \tag{50}$$

$$[D] = [I_{\mathrm{sc},B}] + \sum_{i=1}^{N}(I_{s_{i,2}}\hat{\boldsymbol{s}}_{i,2} + m_{\mathrm{sp}_i}d_i[\tilde{\boldsymbol{r}}_{S_{c,i}/B}]\hat{\boldsymbol{s}}_{i,3})\boldsymbol{b}_{\theta_i}^T \tag{51}$$

$$\boldsymbol{v}_{\mathrm{trans}} = m_{\mathrm{sc}}\ddot{\boldsymbol{r}}_{C/N} - 2m_{\mathrm{sc}}[\tilde{\boldsymbol{\omega}}_{\mathcal{B}/\mathcal{N}}]\boldsymbol{c}' - m_{\mathrm{sc}}[\tilde{\boldsymbol{\omega}}_{\mathcal{B}/\mathcal{N}}][\tilde{\boldsymbol{\omega}}_{\mathcal{B}/\mathcal{N}}]\boldsymbol{c} - \sum_{i=1}^{N}(m_{\mathrm{sp}_i}d_i\dot{\theta}_i^2\hat{\boldsymbol{s}}_{i,1} + m_{\mathrm{sp}_i}d_ic_{\theta_i}\hat{\boldsymbol{s}}_{i,3}) \tag{52}$$

$$\boldsymbol{v}_{\mathrm{rot}} = -\sum_{i=1}^{N}\{(\dot{\theta}_i[\tilde{\boldsymbol{\omega}}_{\mathcal{B}/\mathcal{N}}] + c_{\theta_i}[I_{3\times3}])(I_{s_{i,2}}\hat{\boldsymbol{s}}_{i,2} + m_{\mathrm{sp}_i}d_i[\tilde{\boldsymbol{r}}_{S_{c,i}/B}]\hat{\boldsymbol{s}}_{i,3}) + m_{\mathrm{sp}_i}d_i\dot{\theta}_i^2[\tilde{\boldsymbol{r}}_{S_{c,i}/B}]\hat{\boldsymbol{s}}_{i,1}\} - [\tilde{\boldsymbol{\omega}}_{\mathcal{B}/\mathcal{N}}][I_{\mathrm{sc},B}]\boldsymbol{\omega}_{\mathcal{B}/\mathcal{N}} - [I'_{\mathrm{sc},B}]\boldsymbol{\omega}_{\mathcal{B}/\mathcal{N}} + \boldsymbol{L}_B \tag{53}$$

Equation (48) represents a system of six linear equations that can solve the Schur complement matrix formulation for the partitioned form of the hub system mass matrix:

$$\dot{\boldsymbol{\omega}}_{\mathcal{B}/\mathcal{N}} = ([D] - [C][A]^{-1}[B])^{-1}(\boldsymbol{v}_{\mathrm{rot}} - [C][A]^{-1}\boldsymbol{v}_{\mathrm{trans}}) \tag{54}$$

$$\ddot{\boldsymbol{r}}_{B/N} = [A]^{-1}(\boldsymbol{v}_{\mathrm{trans}} - [B]\dot{\boldsymbol{\omega}}_{\mathcal{B}/\mathcal{N}}) \tag{55}$$

The remaining step is to solve for the solar panel accelerations $\ddot{\theta}_i$. The solutions for $\dot{\boldsymbol{\omega}}_{\mathcal{B}/\mathcal{N}}$ and $\ddot{\boldsymbol{r}}_{B/N}$ found in Eqs. (54) and (55) are backsubstituted into the simplified solar panel motion EOM [Eq. (41)]. This manipulation avoids having to use an inverse with a size of $N_s + 6$ to solve the $N_s + 6$ coupled differential equations. The equations presented for the backsubstitution method only require two 3×3 inverses. This can dramatically increase the computational speed of a computer simulation because matrix inverse calculations scale a cube the size of the matrix. Additionally, this modularizes the EOMs because the software does not need to populate a system mass matrix with correct locations with respect to other state variables. This can be very beneficial when designing the software architecture for the dynamics.

V. Numerical Simulation

To verify the spacecraft EOMs developed in this Note are agreeing with physics and to provide an example of the flexing behavior, a simulation of a spacecraft similar to the one in Fig. 1 is presented. The hub is a cylinder with its center of mass located at the geometric center of the cylinder. It has two identical solar panels modeled as rectangular prisms located opposite from each other. There are two

Table 1 Simulation parameters for the flexing model (DCM, direction cosine matrix)

Parameter	Notation	Value	Units
Number of solar panels	N_{sp}	2	— —
Total spacecraft mass	m_{sc}	950	kg
Hub mass	m_{hub}	750	kg
Solar panel mass	$m_{\mathrm{sp},i}$	100	kg
Hub inertia matrix about hub center of mass	${}^{\mathcal{B}}[I_{\mathrm{hub},B_c}]$	${}^{\mathcal{B}}\begin{bmatrix} 499.92 & -1.76 & -2.81 \\ -1.76 & 400.01 & -1.12 \\ -2.81 & -1.12 & 350.08 \end{bmatrix}$	kg · m^2
Hub center of mass location with regard to B	${}^{\mathcal{B}}\boldsymbol{r}_{B_c/B}$	${}^{\mathcal{B}}[0 \quad -0.21 \quad 0]^T$	m
Hinge 1 location vector	${}^{\mathcal{B}}\boldsymbol{r}_{H_1/B}$	${}^{\mathcal{B}}[0.5 \quad 1.0 \quad 0.0]^T$	m
Hinge 2 location vector	${}^{\mathcal{B}}\boldsymbol{r}_{H_2/B}$	${}^{\mathcal{B}}[0.5 \quad -1.0 \quad 0.0]^T$	m
Body to hinge 1 DCM	$[H_1B]$	$\begin{bmatrix} -1 & 0 & 0 \\ 0 & 0 & 1 \\ 0 & 1 & 0 \end{bmatrix}$	— —
Body to hinge 2 DCM	$[H_2B]$	$\begin{bmatrix} 1 & 0 & 0 \\ 0 & 0 & -1 \\ 0 & -1 & 0 \end{bmatrix}$	— —
Center of mass offset of solar panel	d_i	1.5	m
Torsional linear spring constant	k_i	300	(N · m)/rad
Torsional linear damping constant	c_i	0	(N · m · s)/rad

Table 2 Simulation parameters for the rigid model

Parameter	Notation	Value	Units
Total spacecraft mass	m_{sc}	950	kg
Hub inertia matrix about hub center of mass	${}^{\mathcal{B}}[I_{\mathrm{hub},B_c}]$	${}^{\mathcal{B}}\begin{bmatrix} 857.81 & -1.76 & -2.81 \\ -1.76 & 1300.01 & -1.12 \\ -2.81 & -1.12 & 1407.97 \end{bmatrix}$	kg · m^2
Hub center of mass location with regard to B	${}^{\mathcal{B}}\boldsymbol{r}_{B_c/B}$	${}^{\mathcal{B}}[0 \quad 0 \quad 0]^T$	m

scenarios simulated: one that includes flexing, and one that models the system as a rigid body. The EOMs for the rigid-body model are not included here but can be seen in Ref. [25]. The two simulations are assembled to have the same mass properties when the panels have zero angular deflection. The spacecraft parameters can be seen in Tables 1 and 2. Additionally, the rigid-body simulation is chosen to have the center of mass coincident with the body frame origin, therefore ${}^{\mathcal{B}}\boldsymbol{r}_{B_c/B} = {}^{\mathcal{B}}\boldsymbol{r}_{C/B} = {}^{\mathcal{B}}[0 \quad 0 \quad 0]^T$. This assumption is common in rigid-body dynamics formulations [2,25]. All of the spacecraft state variables start with zero initial values, except for the angular velocity: ${}^{\mathcal{B}}\boldsymbol{\omega}_{\mathcal{B}/\mathcal{N}} = {}^{\mathcal{B}}[5.73 \quad -8.59 \quad 5.73]^T$. It should be noted that the two simulations also have the same initial conditions, allowing the simulations to be directly comparable; the differences between the two simulations are solely due to the impact of flexing. The simulations are given an impulsive body-fixed force of ${}^{\mathcal{B}}\boldsymbol{F}_{\text{ext}} = {}^{\mathcal{B}}[0 \quad 100 \quad 0]^T$ N, from $t = 0$ to $t = 30$ s; for the remainder of the simulation, there are no external forces or torques on the spacecraft.

The results from these simulations can be seen in Figs. 2–4. In Fig. 2, the variables ${}^{\mathcal{N}}\dot{\boldsymbol{r}}_{B/N}$ and ${}^{\mathcal{B}}\boldsymbol{\omega}_{\mathcal{B}/\mathcal{N}}$ are plotted for both the flexing model and rigid-body simulations. The flexing impact on the simulations can readily be seen from these plots and visually shows how this can impact the simulation fidelity and accuracy of simulated accelerometers. Figure 3 shows the angular deflection of each solar panel, and these oscillations are what are driving the oscillations in the translational and rotational motions.

Figure 4 is included to give verification of energy and momentum conservation for the EOMs developed in this Note. The four conservation quantities being considered are orbital angular momentum, orbital energy, rotational angular momentum, and rotational energy. The orbital conservation values are quantities describing the movement of the center of mass of the spacecraft through space, and the rotational conservation quantities are describing the rotation of the spacecraft about its center of mass. Figure 4 shows that the four energy and momentum quantities are conserved after the impulsive force is turned off. This gives confidence in the formulation presented.

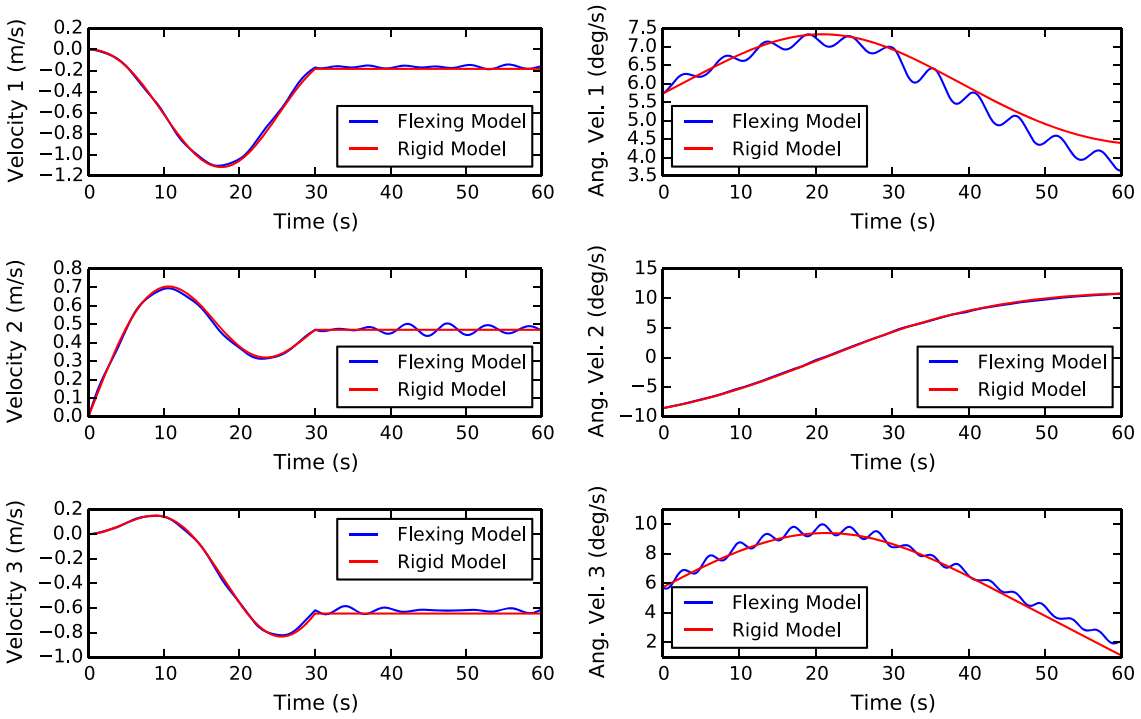

a) Inertial velocity of point B in inertial frame components

b) Inertial angular velocity of body frame in body frame components

Fig. 2 Inertial velocity of point B and inertial angular velocity (Ang. Vel.) of the body frame.

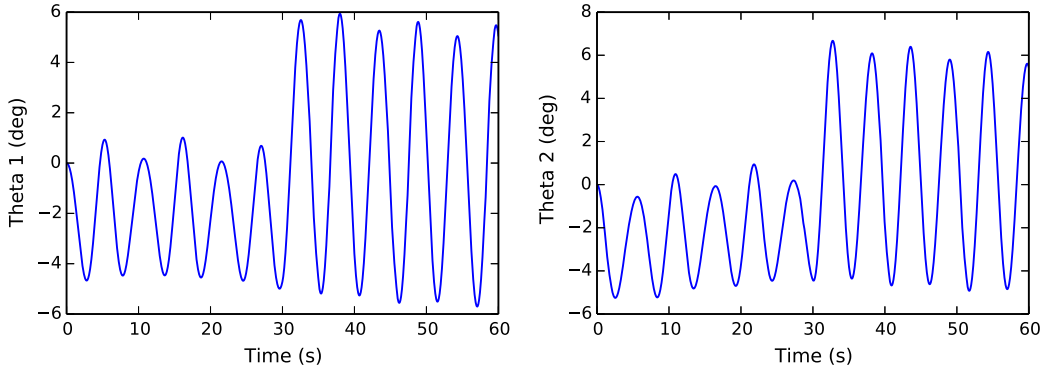

a) Angular deflection of panel 1

b) Angular deflection of panel 2

Fig. 3 Angular deflection of the hinged rigid-bodies.

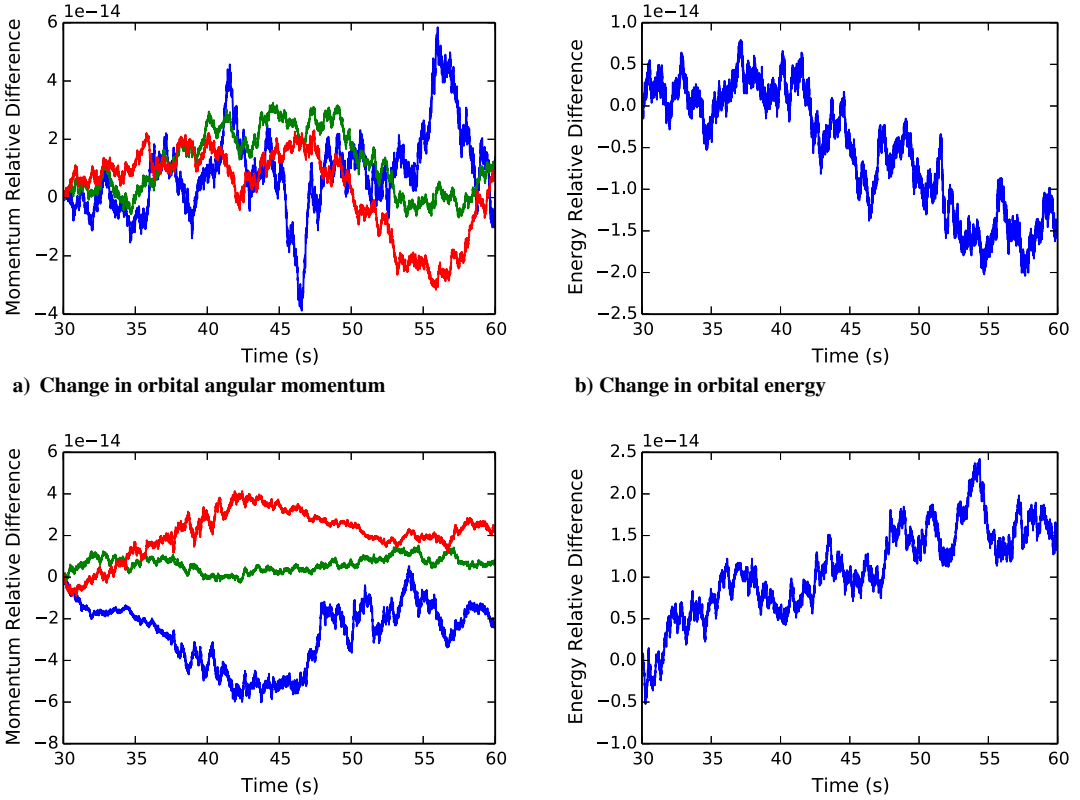

a) Change in orbital angular momentum **b) Change in orbital energy**

c) Change in rotational angular momentum **d) Change in rotational energy**

Fig. 4 Conservation of angular momentum and energy.

VI. Conclusions

This Note presents a compact, frame independent formulation for a first-order approximation of flexible dynamics that can be applied to spacecraft with appended solar panels or hinged structural subcomponents that can be modeled as single rigid bodies. The numerical results show the impact of flexing and the need for it to be included in simulations if large external forces are present to excite panel deflections. Also, the conservation of momentum and energy results that are provided show that the formulation is agreeing with physics and gives verification of the model. Additionally, the backsubstitution method presented is more computationally efficient because it removes the need for a fully coupled system mass matrix inverse. Modeling the flexing effect using this model is an excellent way to analyze the impact of flexing on the spacecraft by running simulations through the life of missions and narrow down scenarios susceptible to unwanted flexing behavior.

References

[1] Banerjee, A. K., "Contributions of Multibody Dynamics to Space Flight: A Brief Review," *Journal of Guidance, Control, and Dynamics*, Vol. 26, No. 3, 2003, pp. 385–394. doi:10.2514/2.5069

[2] Sidi, M., *Spacecraft Dynamics and Control: A Practical Engineering Approach*, Cambridge Aerospace Series, Cambridge Univ. Press, New York, 1997, pp. 291–298, Chap. 10. doi:10.1017/CBO9780511815652

[3] Aslanov, V. S., and Yudintsev, V. V., "Dynamics, Analytical Solutions and Choice of Parameters for Towed Space Debris with Flexible Appendages," *Advances in Space Research*, Vol. 55, No. 2, 2015, pp. 660–667, http://www.sciencedirect.com/science/article/pii/S0273117714006620 [retrieved 2018].

[4] Junkins, J., and Kim, Y., *Introduction to Dynamics and Control of Flexible Structures*, AIAA Education Series, AIAA, Washington, D.C., 1993.

[5] Modi, V. J., "Attitude Dynamics of Satellites with Flexible Appendages—A Brief Review," *Journal of Spacecraft and Rockets*, Vol. 11, No. 11, 1974, pp. 743–751. doi:10.2514/3.62172

[6] Angeles, J., and Kecskeméthy, A., *Kinematics and Dynamics of Multi-Body Systems*, Vol. 360, Springer, New York, 2014, pp. 95–108. doi:10.1007/978-3-7091-4362-9

[7] Fleischer, G. E., and Likins, P. W., "Attitude Dynamics Simulation Subroutines for Systems of Hinge-Connected Rigid Bodies," Jet Propulsion Lab. TR 32-1592, Pasadena, CA, 1970.

[8] Jerkovsky, W., "The Structure of Multibody Dynamics Equations," *Journal of Guidance, Control, and Dynamics*, Vol. 1, No. 3, 1978, pp. 173–182. doi:10.2514/3.55761

[9] Likins, P. W., "Point-Connected Rigid Bodies in a Topological Tree," *Celestial Mechanics*, Vol. 11, No. 3, 1975, pp. 301–317. doi:10.1007/BF01228809

[10] Hooker, W. W., "A Set of r Dynamical Attitude Equations for an Arbitrary n-Body Satellite Having r Rotational Degrees of Freedom," *AIAA Journal*, Vol. 8, No. 7, 1970, pp. 1205–1207. doi:10.2514/3.5873

[11] Kane, T. R., and Levinson, D. A., "Multibody Dynamics," *Journal of Applied Mechanics*, Vol. 50, No. 4b, 1983, pp. 1071–1078. doi:10.1115/1.3167189

[12] Kane, T. R., and Levinson, D. A., "The Use of Kane's Dynamical Equations in Robotics," *International Journal of Robotics Research*, Vol. 2, No. 3, 1983, pp. 3–21. doi:10.1177/027836498300200301

[13] Zarafshan, P., and Moosavian, S. A. A., "Manipulation Control of a Space Robot with Flexible Solar Panels," *2010 IEEE/ASME International Conference on Advanced Intelligent Mechatronics (AIM)*, IEEE Publ., Piscataway, NJ, 2010, pp. 1099–1104.

[14] Moosavian, S. A. A., and Papadopoulos, E., "Explicit Dynamics of Space Free-Flyers with Multiple Manipulators via SPACEMAPLE," *Advanced Robotics*, Vol. 18, No. 2, 2004, pp. 223–244. doi:10.1163/156855304322758033

[15] Kuang, J., Meehan, P. A., Leung, A., and Tan, S., "Nonlinear Dynamics of a Satellite with Deployable Solar Panel Arrays," *International Journal of Non-Linear Mechanics*, Vol. 39, No. 7, 2004, pp. 1161–1179. doi:10.1016/j.ijnonlinmec.2003.07.001

[16] Wallrapp, O., and Wiedemann, S., "Simulation of Deployment of a Flexible Solar Array," *Multibody System Dynamics*, Vol. 7, No. 1, 2002, pp. 101–125.
doi:10.1023/A:1015295720991

[17] Wie, B., Furumoto, N., Banerjee, A., and Barba, P., "Modeling and Simulation of Spacecraft Solar Array Deployment," *Journal of Guidance, Control, and Dynamics*, Vol. 9, No. 5, 1986, pp. 593–598.
doi:10.2514/3.20151

[18] Hu, Q., Shi, P., and Gao, H., "Adaptive Variable Structure and Commanding Shaped Vibration Control of Flexible Spacecraft," *Journal of Guidance, Control, and Dynamics*, Vol. 30, No. 3, 2007, pp. 804–815.
doi:10.2514/1.24441

[19] Xiao, B., Hu, Q., and Zhang, Y., "Adaptive Sliding Mode Fault Tolerant Attitude Tracking Control for Flexible Spacecraft under Actuator Saturation," *IEEE Transactions on Control Systems Technology*, Vol. 20, No. 6, 2012, pp. 1605–1612.
doi:10.1109/TCST.2011.2169796

[20] Zhong, C., Guo, Y., Yu, Z., Wang, L., and Chen, Q., "Finite-Time Attitude Control for Flexible Spacecraft with Unknown Bounded Disturbance," *Transactions of the Institute of Measurement and Control*, Vol. 38, No. 2, 2015, pp. 240–249.
doi:10.1177/0142331214566223

[21] Liu, C., Ye, D., Shi, K., and Sun, Z., "Robust High-Precision Attitude Control for Flexible Spacecraft with Improved Mixed H_2/H_∞ Control Strategy Under Poles Assignment Constraint," *Acta Astronautica*, Vol. 136, July 2017, pp. 166–175, http://www.sciencedirect.com/science/article/pii/S0094576516306701 [retrieved 2018].

[22] Kane, T. R., and Levinson, D. A., "Formulation of Equations of Motion for Complex Spacecraft," *Journal of Guidance, Control, and Dynamics*, Vol. 3, No. 2, 1980, pp. 99–112.
doi:10.2514/3.55956

[23] Forbes, J. R., "Identities for Deriving Equations of Motion Using Constrained Attitude Parameterizations," *Journal of Guidance, Control, and Dynamics*, Vol. 37, No. 4, 2014, pp. 1283–1289.
doi:10.2514/1.G000221

[24] Walsh, A., and Forbes, J. R., "Modeling and Control of Flexible Telescoping Manipulators," *IEEE Transactions on Robotics*, Vol. 31, No. 4, 2015, pp. 936–947.
doi:10.1109/TRO.2015.2441473

[25] Schaub, H., and Junkins, J. L., *Analytical Mechanics of Space Systems*, 3rd ed., AIAA Education Series, AIAA, Reston, VA, 2014.
doi:10.2514/4.102400

[26] Kane, T. R., Likins, P. W., and Levinson, D. A., *Spacecraft Dynamics*, McGraw–Hill, New York, 1983.

[27] Kane, T. R., and Levinson, D. A., *Dynamics, Theory and Applications*, McGraw–Hill, New York, 1985.

D. P. Thunnissen
Associate Editor